Structural Characterization and Cytotoxic Properties of an Apiose-Rich Pectic Polysaccharide Obtained from the Cell Wall of the Marine Phanerogam *Zostera marina*

Vincent Gloaguen,*[,†] Véronique Brudieux,[†,‡] Brigitte Closs,[‡] Aline Barbat,[†] Pierre Krausz,[†] Odile Sainte-Catherine,[§] Michel Kraemer,[§] Emmanuel Maes,[⊥] and Yann Guerardel[⊥]

Laboratoire de Chimie des Substances Naturelles, EA 1069, Faculté des Sciences et Techniques, Université de Limoges, F-87060 SILAB, Saint Viance F-19240, France, Laboratoire d'Oncologie Cellulaire et Moléculaire, EA 3410, Université Paris 13, F-93017, France, and Unité de Glycobiologie Structurale et Fonctionnelle, UMR-CNRS 8576, Université de Lille 1, F-59655, France

Received February 9, 2010

Zosterin, an apiose-rich pectic polysaccharide, was extracted and purified from the sea grass *Zostera marina*. Structural studies conducted by gas chromatography and NMR spectroscopy on a purified zosterin fraction (AGU) revealed a typical apiogalacturonan structure comprising an α-1,4-D-galactopyranosyluronan backbone substituted by 1,2-linked apiofuranose oligosaccharides and single apiose residues. The average molecular mass of AGU was estimated to be about 4100 Da with a low polydispersity. AGU inhibited proliferation of A431 human epidermoid carcinoma cells with an approximate IC_{50} value of 3 μg/mL (0.7 μM). In addition, AGU inhibited A431 cell migration and invasion. Preliminary experiments showed that inhibition of metalloproteases expression could play a role in these antimigration and anti-invasive properties. Autohydrolysis of AGU, which eliminated apiose and oligo-apiose substituents, led to a virtual disappearance of cytotoxic properties, thus suggesting a direct structure−function relationship with the apiose-rich hairy region of AGU.

Plant cell walls are known to be potential sources of pharmacologically active polysaccharides,[1−4] which, within the herbal medicine context, have long been thought of as potential anti-inflammatory and immunostimulatory agents as well as wound-healing promoters.[4] In spite of their ubiquitous presence, carbohydrates and their derivatives were long considered by scientists as molecules having secondary biological importance and playing limited roles such as structural functions (e.g., cellulose) or energy storage (starch, inulin, sucrose). The importance of carbohydrates is now being re-evaluated,[5] and carbohydrate-based therapeutics offer a new class of compounds for controlling various disorders such as cancer, viral infections, and immune dysfunctions.[6−8]

Pectin constitutes one of the three major polysaccharidic components of primary cell walls of plants.[9] The term pectin encompasses a group of acidic heteropolysaccharides with distinct structural domains. Chemical structures of pectins have been thoroughly studied for decades. Like other plant polysaccharides, pectins are polymolecular and polydisperse, exhibiting significant heterogeneity depending on plant source, conditions of extraction, and many other environmental factors. A general pectin model structure has been proposed by Perez and collaborators.[10] To date, apiogalacturonan—a pectic domain characterized by a typical α-1,4-D-galactopyranosyluronan backbone substituted by apiofuranose residues—has been found in a small number of plants. Lemnan is the apiogalacturonan extracted from the duckweed *Lemna minor* L. Its extraction and composition are well documented in the literature.[11−13] The use of lemnan has been proposed for medical, pharmaceutical, and cosmetic applications.[14−18] The lemnan structure comprises an α-1,4-D-galacturonan backbone with apiose side chains grouped within a "hairy" region. A few D-apiose residues appeared to occupy the terminal positions of the macromolecule.[14] Recently, Popov and co-workers[17] suggested that the enhancement of the inflammatory response to lemnan is associated with this apiose-rich hairy region that could then be considered as the active part of the molecule.

* Corresponding author. Tel: (33)555457481. Fax: (33)555457202. E-mail: vincent.gloaguen@unilim.fr.
† Université de Limoges.
‡ SILAB.
§ Université de Paris.
⊥ Université de Lille 1.

In the late 1960s, attention was drawn to *Zostera marina* L., a marine phanerogam,[19−22] which synthesizes an apiose-rich pectic substance named zosterin. Structural studies have been undertaken with the use of specific enzymic[21] and chemical[22] degradations, but the structure of the molecule still remains unknown. The aim of this study was to characterize the structure of zosterin making use of polysaccharide autohydrolysis, i.e., polysaccharide hydrolysis through its own acid groups, and further spectroscopic analyses of the hydrolysis products. Then the effects of both the purified zosterin fraction (named AGU) and apiose-free zosterin on the *in vitro* proliferation, migration, and invasion of human A431 squamous cell carcinoma cells (vulvar epidermoid carcinoma) were investigated in order to characterize the antitumor properties of AGU and to identify the active region of the molecule. The human A431 squamous cell carcinoma cell line represents a good model of an aggressive, highly angiogenic, and metastatic tumor.[23−25] Carcinomas are the most frequent types of human malignancies, and most cancer deaths are related to the formation of metastases. To migrate from the primary tumor, malignant cells degrade the basement membrane and the extracellular matrix before disseminating via blood or lymphatic vessels.[26] We therefore assessed the effects of purified AGU on tumor cell migration and invasion. Because invasion of tumor cells through extracellular matrix involves metalloproteases (MMP), we studied the effects of AGU on the expression of these enzymes.

Results and Discussion

Zosterin, the apiogalacturonan extracted from *Z. marina,* accounts for a significant proportion of the biomass, reaching 11% w/w of dry weight. Analysis of the zosterin crude fraction (Z_c) by GLC of the trimethylsilylated methyl glycoside derivatives showed the presence of high amounts of apiose and galacturonic acid (GalA) that represent up to 47% molar ratio of the total sugars (Table 1). Enzymic and purification processes led to apiose enrichment of the molecule to give an apiogalacturonan fraction (AGU) containing 53.5% apiose and 30.5% GalA. The homogeneity of this fraction was evaluated by high-pressure size exclusion chromatography (HP-SEC). The narrow peak of the chromatogram presented in Figure 1 is characteristic of a homogeneous fraction. Based on colorimetric estimation, the ratio of reducing sugar to total carbohydrate suggests

10.1021/np100092c
Published on Web 05/13/2010

Table 1. Monosaccharide Composition (Molar Ratio) of the Crude (Z_c) and Purified (AGU) Zosterin and Its Fractions Obtained after Autohydrolysis[a]

	Me-Xyl	Api	Ara	Rha	Fuc	Xyl	GalA	Man	Gal	Glc	GlcA
Z_c	t	21.0	3.4	9.4	4.6	17.4	26.3	1.0	5.8	7.2	3.9
AGU	t	53.5	1.9	3.6	1	5.4	30.5	0.2	1.9	0.8	1.2
NRF	t	100	n.d.	n.d.	n.d.	n.d.	n.d.	n.d.	n.d.	n.d.	n.d.
RF	n.d.	t	n.d.	0.8	n.d.	4.2	92.3	n.d.	0.9	1.8	n.d.

[a] Retained (RF) or nonretained (NRF) on DOWEX 1×2 resins. t: trace; nd: not determined. Me-Xyl: methyl xylose; Api: apiose; Ara: arabinose; Rha: rhamnose; Fuc: fucose; Xyl: xylose; GalA: galacturonic acid; Man: mannose; Gal: galactose; Glc: glucose; GlcA: glucuronic acid.

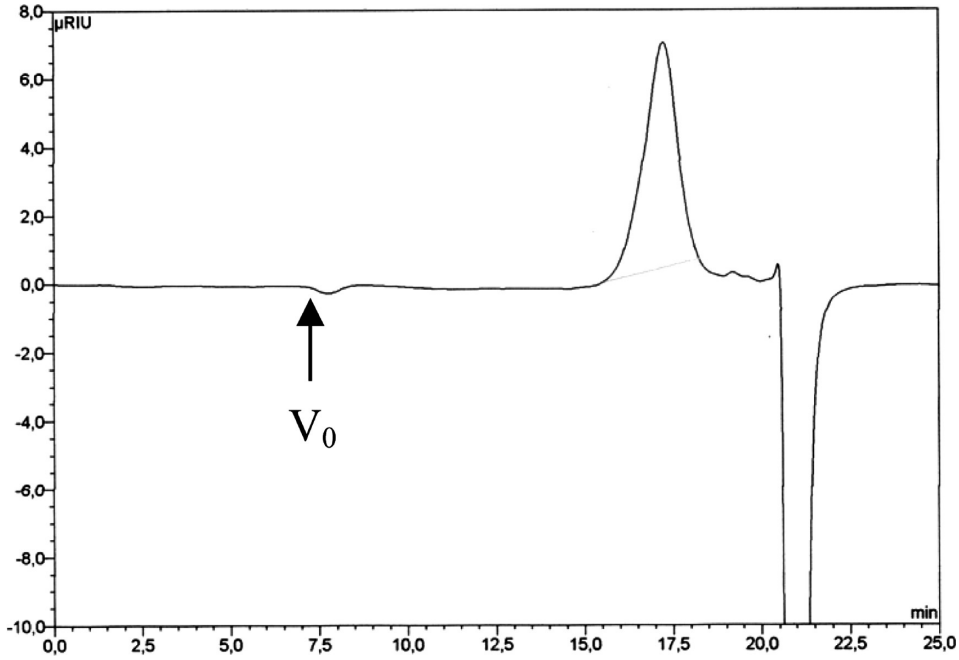

Figure 1. HP-SEC of purified zosterin (AGU). V_0 is the void volume.

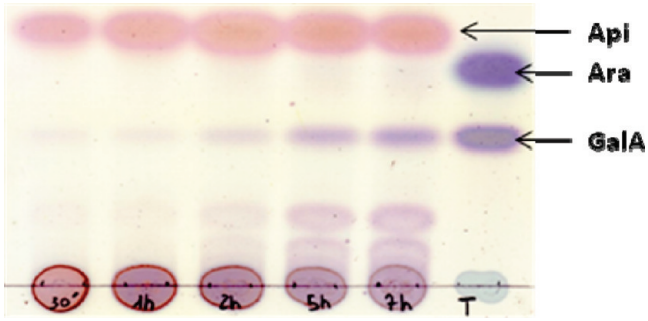

Figure 2. TLC monitoring of AGU autohydrolysis. T*:* standard GalA and Ara; Api: apiose; GalA: galacturonic acid; Ara: arabinose.

that AGU has an average degree of polymerization (DP) of 25, corresponding to a mass close to 4100 Da.

AGU proved unstable to the exposure to acid. The TLC plate showing the kinetics of the reaction (Figure 2) indicates that even a short exposure to acidic conditions degrades the molecule. TLC data therefore suggest the rapid liberation of monosaccharides with characteristic R_f values higher than that of the standard arabinose followed by fragmentation of the homogalacturonic backbone of the molecule, giving oligo-uronides detected by a characteristic blue color after treatment with an acidic orcinol solution. On the basis of the TLC results, we chose one hour as the standard hydrolysis time. The mixture was then purified by anion exchange chromatography on DOWEX 1×2 resin to give a nonretained fraction (NRF) that contained only apiose and a retained fraction (RF) devoid of apiose but containing a high content of galacturonic acid (Table 1). The NRF and RF were further purified by size exclusion chromatography on Biogel P2 using water as the eluent. Homogeneous fractions were separated and subjected to NMR spectroscopic analysis. In particular, the NRF was separated into two different carbohydrate-containing subfractions: NRF1 included the 200−2000 Da fractionation range from gel filtration, and NRF2 eluted at the total column volume, which established that NFR2 exhibits a very low molecular weight.

Structural features of both subfractions NRF1 and NRF2 were established through a combination of homonuclear, one and two-dimensional ^{1}H NMR experiments, and heteronuclear two-dimensional ^{1}H−^{13}C NMR experiments. Proton and carbon spin systems of individual monosaccharides were established by COSY and relayed ^{1}H−^{1}H COSY experiments, as well as ^{1}H−^{13}C HSQC and HSQC-TOCSY experiments. Both vicinal and direct coupling constants, $^3J_{H1,H2}$ and $^1J_{C1,H1}$, were established by ^{1}H−^{1}H COSY and nondecoupled ^{1}H−^{13}C HSQC-NMR experiments, respectively.

As shown in Figure 3, the anomer region of the ^{1}H−^{13}C HSQC-NMR spectrum of NRF2 shows four major sharp signals assigned to the individual monosaccharides labeled **1** to **4**. NMR parameters (Table 2) of all four compounds perfectly fit with the parameters of a mixture of synthetic free apiose conformers.[27] Indeed, previous work established that free D-apiose (3-*C*-(hydroxymethyl)-D-*glycero*-tetrose) was naturally occurring in solution as a mixture of the α/β and D/L furanoses in proportions similar to those observed in NRF2 (Figure 3), which unambiguously demonstrates that this fraction mainly contains free apiose. In accordance with the composition analysis of the NRF fraction by GC, the NMR experiments also permitted identification of α/β isomers of free Xyl and methyl-Xyl residues (data not shown). Altogether, NMR data established that NRF2 is comprised of 80% free apiose, in accordance with its overall low mobility in gel filtration.

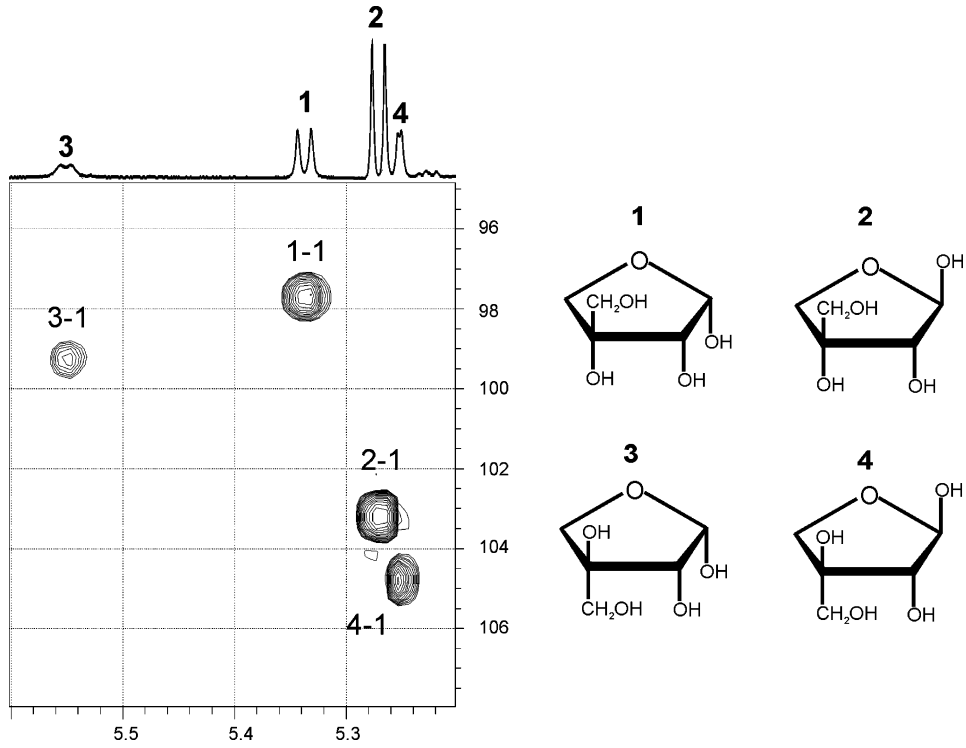

Figure 3. NMR analysis of NRF2. (Left) $^{1}H-^{13}C$ HSQC-NMR spectrum of free D-apiose in NRF2. (Right) The four furanose forms of D-apiose in solution, according to Snyder and Serianni.[27] **1**, 3-(C-hydroxymethyl)-α-D-erythrofuranose; **2**, 3-(C-hydroxymethyl)-β-D-erythrofuranose; **3**, 3-(C-hydroxymethyl)-β-L-threofuranose; and **4**, 3-(C-hydroxymethyl)-α-L-threofuranose. These four molecules are referred to as α-D-apiose, β-D-apiose, β-L-apiose, and α-L-apiose respectively.

Table 2. ^{1}H and ^{13}C NMR Chemical Shift (ppm) Assignments of Free Apiose Residues in NRF1

	$^{1}H/^{13}C$ (ppm)			
cpd (ratios)	H-1/C-1	H-2/C-2	$^{3}J_{H1,H2}$ (Hz)	$^{1}J_{C1,H1}$ (Hz)
1 (1)	5.34/97.6	3.98/72.7	4.8	172
2 (2)	5.27/103.1	3.87/78.5	4.5	171
3 (0.5)	5.55/99.1	3.97/75.4	3.8	173
4 (1)	5.24/104.7	4.02/81.6	1.32	171

Table 3. ^{1}H and ^{13}C NMR Chemical Shift (ppm) Assignments of Apiose Residues from Oligomers in NRF2

	$^{1}H/^{13}C$ (ppm)				
cmpd	H-1/C-1	H-2/C-2	C-3	H-4,4′/C-4	H-5,5′/C-5
a	5.7/104.8	4.1/83.0	84.0	3.9−3.7/73.1	3.8−3.7/63.6[a]
b	5.6/104.0	4.0/77.8	87.6	3.7−3.6/65.5	3.5−3.5/64.8
c	5.3/104.2	4.0/85.0	80.7	3.9−3.8/75.3	3.7−3.6/65.5[a]

[a] Sets of values may be exchanged.

In contrast to NRF2, the anomer region of the NRF1 NMR spectra showed three major heterogeneous signals between 5.2 and 5.8 ppm labeled **a** to **c**, all of them attributed to anomers of D-apiose residues, in agreement with their ^{1}H and ^{13}C spin systems (Table 3). Each signal results from the combination of numerous subsignals presenting slightly different ^{1}H and ^{13}C NMR shifts that are indicative of the presence of a polydisperse molecule. However, spin systems derived from the **a**−**c** broad signals are sufficiently homogeneous to deduce that their individual subsignals are associated with monosaccharides presenting identical linkage patterns. A $^{1}H-^{13}C$ HSQC-TOCSY NMR experiment (Figure 4) established that **a** and **c** correspond to substitution at the C-2 position, according to their unshielded H-2/C-2 shifts, 4.1/83.0 and 4.0/85.0 ppm respectively, whereas the **b** $^{1}H/C^{13}$ spin system established that the corresponding residue does not bear any substituent. All three **a**−**c** C-5 carbons were observed between 63.6 and 65.5 ppm, ruling out substitution of the C-5 position of **a**−**c**, contrary to the pectic polysaccharide of the duckweed *L. minor* L.[13] Thus, altogether NMR data established that NRF2 is mainly constituted by a mixture of C-2-linked D-apiose oligomers presenting an average of five monosaccharide residues, as established by differential integration of ^{1}H NMR signals. The spin system of **c** strongly suggests that it consists of a mixture of reducing D-apiose isomers **1**, **2**, and **3**, all presenting a deshielded C-2 at 85.0 ppm indicative of a C-2-linkage. The spin system of the fourth isomer of the reducing D-apiose residue (isomer **4**) was then identified from a minor anomer signal at δ 5.63 (data not shown). Although comparison of the observed NMR parameters with data from the literature[13,14] strongly suggests that internal and external nonreducing **a** and **b** compounds are β-D-Api residues, definitive conformations should be established by analyzing synthetic conformers of 1,2- linked oligomers of D-apiose.

According to the general structural model proposed for the duckweed *L. minor* L. apiogalacturonan[13] and taking into account the results obtained in the present study, we proposed the following structural model for *Z. marina* apiogalacturonan:

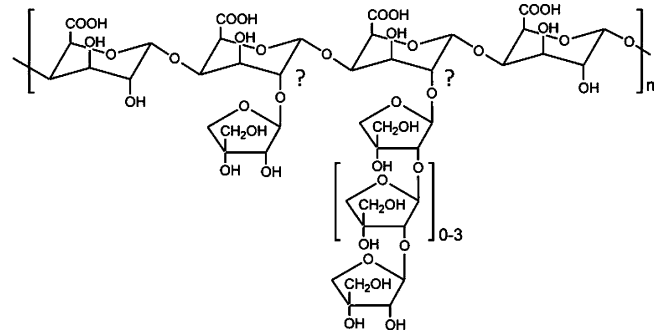

The nature of the linkages of apiose and apio-oligosaccharides with the galacturonan as well as their distribution along the backbone remains to be specified.

To investigate the effects of AGU and RF on cell proliferation, tumor cells were treated with increasing doses of both fractions

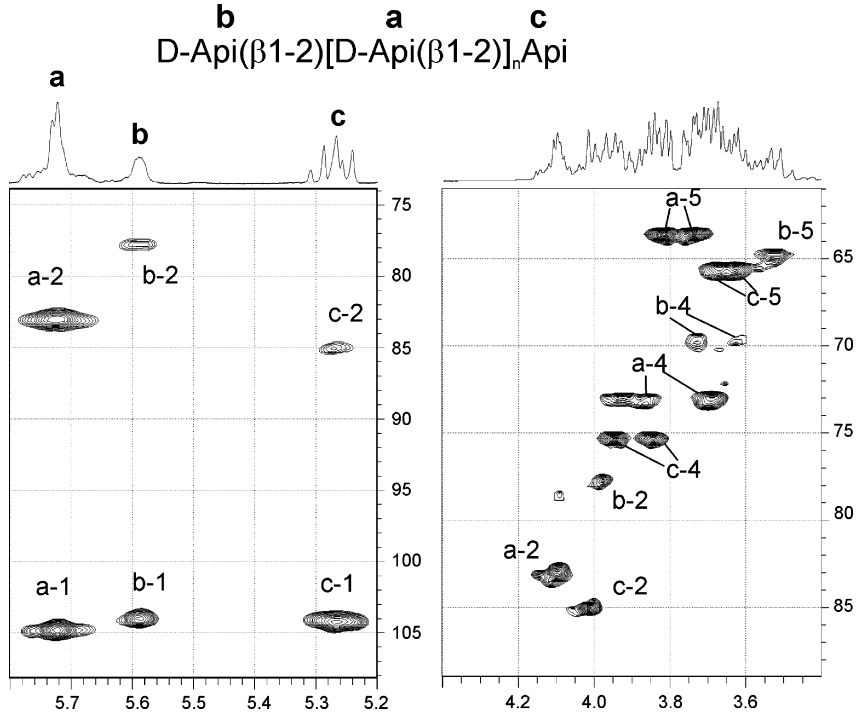

Figure 4. NMR analysis of NRF1. (Left) Anomer region of $^{1}H-^{13}C$ HSQC-TOCSY-NMR spectrum. (Right) Bulk region of the $^{1}H-^{13}C$ HSQC-NMR spectrum of apiose oligomers.

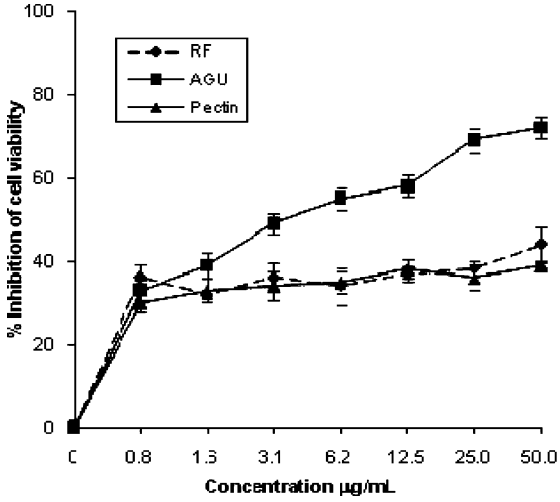

Figure 5. Dose-dependent effects of AGU, RF fraction and standard commercial pectin (Sigma) on A431 cell viability. A431 cells were treated with increasing concentrations (0.8 to 50 μg/mL) of AGU, RF fraction and pectin for 72 h. Results are mean ± SEM of three independent experiments.

ranging from 0.8 to 50 μg/mL. Both fractions inhibited A431 cell proliferation (Figure 5). AGU inhibited cell proliferation in a dose-dependent manner, and the IC_{50} was 3 μg/mL. The maximal inhibition of A431 cell proliferation with the RF or commercial pectin (e.g., polygalacturonic acid from citrus, Sigma) was 44% or 39%, respectively, at 50 μg/mL. Further experiments were carried out with the most potent fraction, AGU.

In the presence of fetal calf serum as a chemotactic stimulus in the lower part of the Boyden migration chamber, A431 cells migrated through the pores to the lower surface of the membrane. AGU significantly reduced cell migration (Figure 6). Compared with untreated control cells, migration of A431 decreased by 80% and 60% with AGU at 25 and 6 μg/mL, respectively.

A Matrigel invasion assay was performed to study the effects of AGU (25 and 6 μg/mL) on the invasive ability of A431 cells (Figure 7). Compared with untreated control cells, invasion of A431 through Matrigel significantly decreased by 90% ($p < 0.05$) and 65% ($p < 0.05$) in the presence of 25 and 6 μg/mL AGU, respectively.

Cell migration that takes place during angiogenesis requires degradation of the extracellular matrix by matrix metalloproteases (MMP).[27] Because AGU inhibited migration and invasion of A431 cells, we then examined by zymography whether this compound could affect the expression of MMP9 and MMP2 gelatinases by A431 cells. Analysis by quantitative zymography (Figure 8) after 72 h of treatment with AGU at 6 μg/mL revealed that the expression of ProMMP9, MMP9, and ProMMP2 decreased respectively by 20%, 45%, and 25%. AGU at 25 μg/mL inhibited the expression of ProMMP9, MMP9, and ProMMP2, respectively, by 20%, 65%, and 45% as compared to control cells. Inhibition of cell invasion observed in Boyden chambers with AGU clearly occurred via an inhibition of MMP expression.

Pectinase digestion of zosterin produced a pectinase-resistant apiogalacturonan (AGU) and a mixture of oligogalacturonide and galacturonic acid, evidencing the presence of the typical homogalacturonan part of pectin within the macromolecule. Similar results have been obtained by Ovodov et al.[21] with lemnan. AGU, mainly composed of apiose and galacturonic acid, proved to be quite homogeneous by HP-SEC. Autohydrolysis of AGU released apiose side chains (apiose and oligoapiose chains). The zosterin oligoapiose D-Api-(β1,2)$_n$-D-Api-(β1, ...) is different from the apiodisaccharide D-Api-(β1,5)-D-Api-(β1, ...) proposed by Golovchenko et al.[13] for lemnan. We demonstrated that AGU from zosterin presents high, dose-dependent, cytotoxic activity against A431 carcinoma cells. The RF fraction obtained by autohydrolysis of AGU, which is completely devoid of apiose, failed to mediate cytotoxic activity and had an activity similar to that obtained with commercial pectin exclusively composed of galacturonic acid. These data suggest that the apiose side chains in the hairy region of zosterin play an important role in the observed cytotoxic activity. The data obtained reveal a close structure−function relationship, which complements former studies[16,17] on the anti-inflammatory effect of lemnan and is in good agreement with previous data that demonstrated the direct involvement of the hairy region of bioactive pectin.[4,29,30]

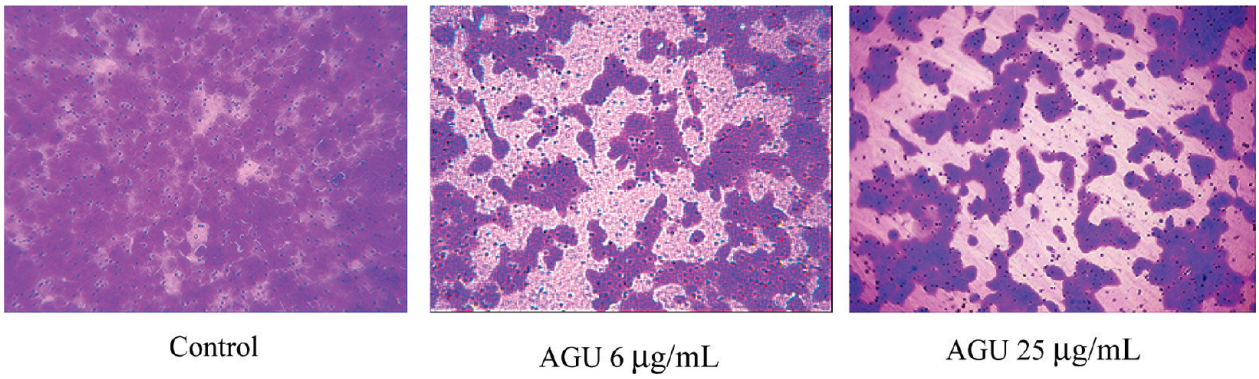

Figure 6. Effects of AGU on the migration of A431 cells. Original magnification ×200.

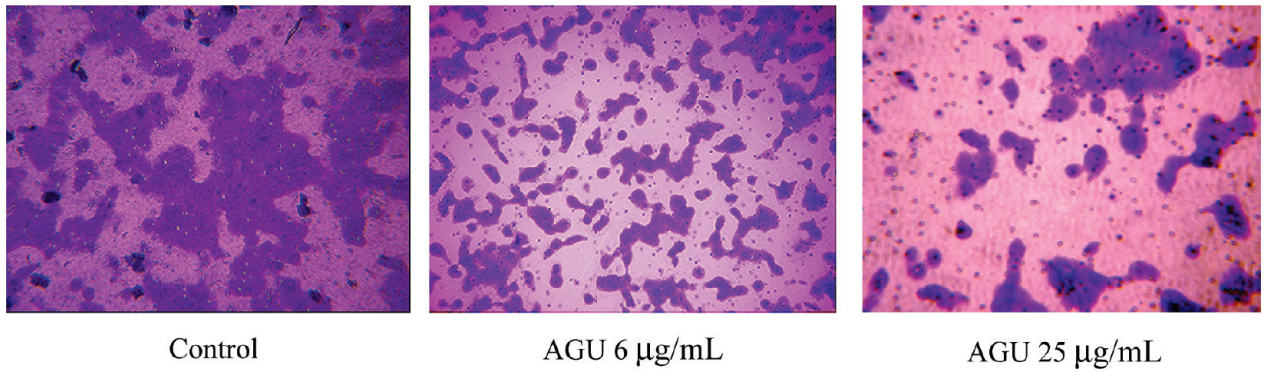

Figure 7. Effects of AGU on the invasion of A 431 cells. Original magnification ×200.

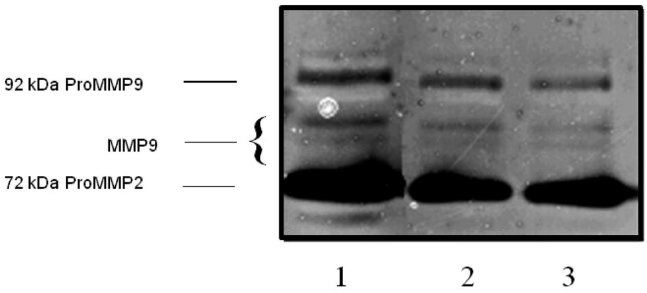

Figure 8. Effects of AGU on ProMMP9, MMP9, and ProMMP2 expression by A431 cells. Lane 1, nontreated A431 cells; lane 2, AGU-treated A431 cells (6 μg/mL); lane 3, AGU-treated A431 cells (25 μg/mL).

The present work demonstrates that zosterin inhibits proliferation, invasion, and migration of highly invasive A431 human tumor cells. Regarding the underlying mechanism, we propose that the AGU fraction can act, at least partly, via an inhibition of MMP expression.

Experimental Section

General Experimental Procedures. ^{1}H (400.33 MHz) and ^{13}C (100.66 MHz) NMR spectra were recorded on a Brüker 9.39 T Avance spectrometer (Centre Commun de Mesure RMN de Lille). The spectrometer was equipped with a 5 mm broad band inverse probehead with z-gradients. Separation of *per*-trimethyl-silylated methylglycosides was done with a Perichrom gas chromatograph fitted with a flame-ionization detector. A CPSIL-5CB (Chrompack, 0.32 mm ×50 m) capillary column was used with the following temperature program: 120−240 at 2 °C/min; nitrogen was the carrier gas at 0.5 atm. All extracts (see below) were evaporated below 40 °C under reduced pressure. Centrifugations were conducted at 10 000 rpm for 15 min at 25 °C. Total carbohydrate was measured by the phenol sulfuric acid method.[31] Hexuronic acids were determined with the *meta*-hydroxydiphenyl method.[32] Reducing sugar contents were estimated according to Lever.[33]

Plant Material. *Zostera marina* L., identified by Dr. G. Saladin, at the University of Limoges, was collected in the Swedish Kattegat (Baltic Sea). A voucher specimen was deposited at the Life Sciences Department of the Limoges University under the reference Zm06-2006.

Isolation and Purification of Zosterin. Lyophilized *Z. marina* biomass was ground. Ten grams of the resulting powder was consecutively left overnight in 50 mL of acetone and washed several times with acetone and EtOH, until the filtrate became clear. The dried powder was heated at 70 °C in 200 mL of 1% (w/v) ammonium oxalate solution for 2 h. The resulting supernatant was recovered after centrifugation (5000*g*, 15 min), dialyzed against H_2O (Spectrapor MWCO 6-8000), and lyophilized to produce the crude zosterin fraction (Z_c).

About one gram of Z_c was solubilized in distilled H_2O and subjected to pectinase digestion (pectinase from *Aspergillus niger*, Sigma; 0.2% v/v, 1 h at 37 °C). The mixture was then heated and left to boil for 1 min; the coagulated proteins were removed by centrifugation (5000*g*, 15 min). The supernatant was finally precipitated by addition of three volumes of EtOH; the pellet was recovered after centrifugation, solubilized in H_2O, dialyzed against H_2O (Spectrapor MWCO 6-8000), and lyophilized to produce the purified apiogalacturonan fraction (AGU).

Monosaccharide Composition. The monosaccharide composition was carried out after methanolysis (MeOH/HCl 0.5 N, 24 h, 80 °C) by GC analysis of the *per*-trimethyl-silylated methylglycosides according to Kamerling et al.,[34] modified by Montreuil et al.[35]

Mass Polydispersity. Mass polydispersity of zosterin was studied by high-pressure size exclusion chromatography (HP-SEC) with a Dionex apparatus equipped with a refractive index detector. Zosterin solution at a concentration of 1 mg/mL was deposited onto a set of two serially coupled 250 × 8 mm mixed Aquagel-OH columns (Polymer Laboratories); 50 mM $NaNO_3$ was used as eluent at a flow rate of 1 mL/min.

Autohydrolysis of Zosterin. An aqueous solution of the native polysaccharide (0.5% w/v) was converted into its acidic form by filtration through an Amberlite IR 120 (H^+) column and subsequently subjected to autohydrolysis[36] by heating in a sealed tube at 100 °C for 1 h. The reaction course was monitored by TLC on a Kieselgel 60F plate (Merck) using butanol/acetic acid/H_2O (2:1/1 v/v) as eluent. Carbohydrates were then detected by heating at 105 °C after treatment with a 0.1% orcinol (w/v) in 20% aqueous H_2SO_4 (v/v) solution. Oligosaccharides were separated by anion exchange chromatography

with DOWEX 1×2 (Cl^-) resins in batch conditions. The nonretained fraction containing neutral mono- and/or oligosaccharides was obtained after rinsing with H_2O. The acidic retained fraction was desorbed with 0.5 M ammonium formate solution. Purified mono-, oligo-, and polysaccharide fractions were desalted after five successive freeze-drying cycles and purified by size exclusion chromatography on Biogel P2 (Biorad, 70 × 2 cm) with H_2O as eluent prior to NMR analysis.

NMR Analysis. Samples were twice exchanged against ^2D_2O (99.97% deuterium atoms, EurisoTop, St Aubin, France) and put into classical 5 mm BB NMR tubes. Experiments utilized standard Brüker pulse sequences and parameters; delays and pulses have been optimized for each experiment. The chemical shifts were calibrated using acetone as an internal standard (δ ^{1}H 2.225 and δ ^{13}C 31.55) at 300 K. The mixing time was 80 ms for the HSQC-TOCSY experiment. HMBC was optimized for $^3J_{C,H} \approx$ 7 Hz, corresponding to an evolution delay of 70 ms.

Zosterin Solubilization. The zosterin stock solution was prepared at 1 mg/mL in H_2O. Dilutions were made with Eagle's medium, and the highest concentration tested corresponded to 50 μg/mL.

Cell Line and Cell Culture. The human A431 squamous cell carcinoma cells (vulvar epidermoid carcinoma) were cultured in Dulbecco's modified Eagle's medium (DMEM) supplemented with 10% fetal calf serum (FCS), 2 mM L-glutamine, 1 mM sodium pyruvate, and 50 U/mL streptomycin (all obtained from Life Technologies Inc.), at 37 °C in a 5% CO_2 humidified atmosphere. Human A431 squamous cell carcinoma cells were obtained from the American Type Culture Collection.

Cell Viability Experiments. Cell viability was evaluated using the 3-(4,5-dimethylthiazol-2-yl)-2,5-diphenyltetrazolium bromide (MTT) microculture assay,[37−39] based on the ability of mitochondrial enzymes to reduce MTT into purple formazan crystals. Cells were seeded at a density of 5×10^3 in 96-well flat-bottom plates and incubated in complete culture medium for 24 h. The medium was removed and replaced by 2% FCS medium containing increasing concentrations of AGU or RF fractions varying from 0.8 to 50 μg/mL. Commercial pectin (e.g., polygalacturonic acid from citrus, Sigma) was used under the same conditions as the control. After 72 h incubation, the cells were washed with phosphate-buffered saline and incubated with 0.1 mL of MTT (2 mg/mL) for an additional 4 h at 37 °C. The insoluble product was then dissolved by addition of 200 μL of DMSO. Absorbance corresponding to the solubilized formazan pellet was measured at 570 nm using a Labsystems Multiskan MS microplate reader. Concentration−response curves were constructed, and IC_{50} values were determined. All *in vitro* cell experiments (viability, migration, and invasion assays) were carried out at 37 °C in a 5% CO_2 incubator.

Cell Migration Assay. The influence of the AGU fraction on the migration of A431 cells was investigated as described previously[8,38] using Boyden invasion chambers with 8 μm pore size filters coated with 100 μL of fibronectin (100 μg/mL, Santa Cruz Biotechnology, Santa Cruz, CA) and were allowed to stand overnight at 4 °C. Then, 5×10^4 untreated or AGU (6 or 25 μg/mL) pretreated A431 cells were added to each insert (upper chamber). A strong chemoattractant (10% FCS) was added to the lower chamber. After 24 h incubation at 37 °C in a 5% CO_2 incubator, nonmigrated cells were removed by scraping, and migrated cells were fixed in MeOH and stained with hematoxylin. Cells migrating on the lower surface of the filter were counted in 10 fields using a Zeiss microscope. Results were expressed as a percentage relative to controls normalized to 100%. Experiments were performed in triplicate.

Cell Invasion Assay. Cell invasion experiments were performed with Boyden chambers as described above. The inserts were coated with Matrigel membrane matrix (Falcon, Becton Dickinson Labware, Bedford, MA). A431 cells (5×10^4) were added to the upper well of the Boyden chamber, and 10% FCS was added to the lower chamber. Before seeding the upper chamber, the cells were pretreated for 24 h with APE 5 fractions at 6 or 25 μg/mL. After 24 h at 37 °C in a 5% CO_2 incubator, noninvaded cells in the upper chamber were wiped with a cotton swab, and the filters were fixed, stained, and counted. Results were expressed as a percentage relative to controls normalized to 100%. Experiments were performed in triplicate.

Zymography. A431 cells were added at a density of 50×10^4/well into 6-well tissue culture plates in DMEM/10% FCS. Cells were allowed to adhere for 24 h and were then incubated with the AGU fractions (6 or 25 μg/mL). Conditioned media were collected 72 h after the treatments with AGU fractions, normalized to cell number, mixed with nonreducing Laemmli sample buffer, and subjected to 10% SDS-PAGE containing 0.1% (w/v) gelatin. The gels were washed three times at room temperature with a solution containing 2.5% (v/v) Triton X-100 in H_2O and incubated at 37 °C for 24 h in 50 mM Tris/HCl, pH 7.4, 0.2 M NaCl, 5 mM $CaCl_2$, and 0.05% Brij 35. The gels were stained for 60 min with 0.5% (w/v) R-250 Coomassie blue in 30% MeOH (v/v)/10% acetic acid (v/v). ProMMP9, MMP9, and ProMMP2 detection proceeded by direct visualization of white zones on the gels, indicating the gelatinolytic activity of proteinases. Gelatinase activity was quantified using the NIH Image program.

Acknowledgment. We thank Dr. M. Guilloton for help in editing the manuscript.

References and Notes

(1) Srivastava, R.; Kulshreshtha, D. *Phytochemistry* **1989**, *28*, 2877–2883.
(2) Gloaguen, V.; Krausz, P. *SÖFW J.* **2004**, *130*, 20–26.
(3) Franz, G. *ACS Symp. Ser. 691 (Phytomedicine of Europe)* **1998**, 74–82.
(4) Paulsen, B. S. *Curr. Org. Chem.* **2001**, *5*, 939–950.
(5) Paulsen, B. S. *Phytochem. Rev.* **2002**, *1*, 379–389.
(6) Garbacki, N.; Gloaguen, V.; Bodart, P.; Damas, J.; Tits, M.; Angenot, L. *J. Ethnopharmacol.* **1999**, *68*, 235–241.
(7) Schepetkin, I. A.; Quinn, M. T. *Int. Immunopharmacol.* **2006**, *6*, 317–333.
(8) Moine, C.; Krausz, P.; Chaleix, V.; Sainte-Catherine, O.; Kraemer, M.; Gloaguen, V. *J. Nat. Prod.* **2007**, *70*, 60–66.
(9) Carpita, N. C.; Gibeaut, D. M. *Plant* **1993**, *3*, 1–30.
(10) Perez, S.; Rodriguez-Carvajal, M. A.; Doco, T. *Biochimie* **2003**, *85*, 109–121.
(11) Kindel, P. K.; Cheng, L.; Ade, B. *Phytochemistry* **1995**, *41*, 719–723.
(12) Cheng, L.; Kindel, P. K. *Carbohydr. Res.* **1997**, *301*, 205–212.
(13) Golovchenko, V. V.; Ovodova, R. G.; Shashkov, A. S.; Ovodov, Y. S. *Phytochemistry* **2002**, *60*, 89–97.
(14) Ovodova, R. G.; Golovchenko, V. V.; Shashkov, A. S.; Popov, S.; Ovodov, Y. S. *Russ. J. Bioorg. Chem.* **2000**, *26*, 669–676.
(15) Khasina, E. I.; Sgrebneva, M.; Ovodova, R. G.; Golovchenko, V. V.; Ovodov, Y. S. *Dokl. Biol. Sci.* **2003**, *390*, 204–206.
(16) Popov, S. V.; Golovchenko, V. V.; Ovodova, R. G.; Smirnov, V. V.; Khramova, D. S.; Popova, G. Y.; Ovodov, Y. S. *Vaccine* **2006a**, *24*, 5413–5419.
(17) Popov, S. V.; Ovodova, R. G.; Ovodov, Y. S. *Phytother. Res.* **2006b**, *20*, 403–407.
(18) Dal Farra, C.; Domloge, N.; Peyronnel, D. Patent FR2838962, 2003.
(19) Ovodova, R. G.; Vas'Kovskii, V. E.; Ovodov, Y. S. *Carbohydr. Res.* **1968**, *6*, 328–332.
(20) Ovodova, R. G.; Ovodov, Y. S. *Carbohydr. Res.* **1969**, *10*, 387–390.
(21) Ovodov, Y. S.; Mikheiskaya, L. V.; Ovodova, R. G.; Krasikova, I. N. *Carbohydr. Res.* **1971a**, *18*, 311–318.
(22) Ovodov, Y. S.; Mikheiskaya, L. V.; Ovodova, R. G.; Krasikova, I. N. *Carbohydr. Res.* **1971b**, *18*, 319–322.
(23) Di Benedetto, M.; Starzec, A.; Vassy, R.; Perret, G. Y.; Crépin, M.; Kraemer, M. *Br. J. Cancer* **2003**, *88*, 1987–1994.
(24) Guenin, E.; Ledoux, D.; Oudar, O.; Lecouvey, M.; Kraemer, M. *Anticancer Res.* **2005**, *25*, 1139–1145.
(25) Hamma-Kourbali, Y.; Di Benedetto, M.; Ledoux, D.; Oudar, O.; Leroux, Y.; Lecouvey, M.; Kraemer, M. *Biochem. Biophys. Res. Commun.* **2003**, *310*, 816–23.
(26) Mori, A.; Shigeki, A.; Furutani, M.; Hanaki, K.; Tadeka, Y.; Moriga, T.; Kondo, Y.; Gorin Rivas, M. J.; Imamura, M. *Int. J. Cancer.* **1999**, *80*, 738–743.
(27) Snyder, J. R.; Serianni, A. S. *Carbohydr. Res.* **1987**, *166*, 85–99.
(28) Heissig, B.; Hattori, K.; Friedrich, M.; Rafii, S.; Werb, Z. *Curr. Opin. Hematol.* **2003**, *10*, 136–141.
(29) Paulsen, B. S.; Barsett, H. *Adv. Polym. Sci.* **2005**, *186*, 69–101.
(30) Sakurai, M. H.; Matsumoto, T.; Kiyohara, H.; Yamada, H. *Immunology* **1999**, *97*, 540–547.
(31) Dubois, M.; Gilles, K. A.; Hamilton, J. K.; Rebers, P. A.; Smith, F. *Anal. Chem.* **1956**, *28*, 350–356.
(32) Blumenkrantz, N.; Asboe-Hansen, G. *Anal. Biochem.* **1973**, *54*, 484–489.
(33) Lever, M. *Anal. Biochem.* **1972**, *47*, 273–279.
(34) Kamerling, J. P.; Gerwig, G. J.; Vliegenhart, J. F. G.; Clamp, J. R. *Biochem. J.* **1975**, *151*, 491–495.
(35) Montreuil, J.; Bouquelet, S.; Debray, H.; Fournet, B.; Spik, G.; Strecker, G. In *Carbohydrate Analysis: A Practical Approach*; Chaplin, M. F., Kennedy, J. F., Eds.; IRL Press: Oxford, 1986; pp 143−204.
(36) Ciancia, M.; Cerezo, A. S. *Ciênc. Cultura* **1993**, *45*, 54–61.
(37) Mosmann, T. *J. Immunol. Methods* **1983**, *65*, 55–63.
(38) Neaud, V.; Faouzi, S.; Guirouilh, J.; Le Bail, B.; Balabaud, C.; Bioulac-Sage, P.; Rosenbaum, J. *J. Hepatol.* **1997**, *26*, 1458–1466.
(39) Witczak, Z. J.; Kaplon, P.; Dey, P. M. *Carbohydr. Res.* **2003**, *338*, 11–18.

NP100092C